RESEARCH ARTICLE

Different agonists induce distinct single-channel conductance states in TRPV1 channels

Jesús Aldair Canul-Sánchez[1]*, Ileana Hernández-Araiza[1]*, Enrique Hernández-García[1], Itzel Llorente[1], Sara L. Morales-Lázaro[1], León D. Islas[2], and Tamara Rosenbaum[1]

The TRPV1 ion channel is a membrane protein that is expressed in primary afferent nociceptors, where it is activated by a diverse array of stimuli. Our prior work has shown that this channel is activated by lysophosphatidic acid (LPA), an unsaturated lysophospholipid that is produced endogenously and released under certain pathophysiological conditions, resulting in the sensation of pain. Macroscopic currents activated by saturating concentrations of LPA applied to excised membrane patches are larger in magnitude than those activated by saturating concentrations of capsaicin, which causes near-maximal TRPV1 open probability. Here we show that activation of TRPV1 by LPA is associated with a higher single-channel conductance than activation by capsaicin. We also observe that the effects of LPA on TRPV1 are not caused by an increase in the surface charge nor are they mimicked by a structurally similar lipid, ruling out the contribution of change in membrane properties. Finally, we demonstrate that the effects of LPA on the unitary conductance of TRPV1 depend upon the presence of a positively charged residue in the C terminus of the channel, suggesting that LPA induces a distinct conformational change.

Introduction

Phospholipids, such as phosphatidylinositol 4,5-bisphosphate (PIP_2) and other lipid molecules, have arisen as modulators of the activity of several types of ion channels (Hille et al., 2015). Actions on their target molecules are exerted by either direct interaction or binding and/or through the modulation of second messenger pathways, which in turn regulate ion channel function.

Lysophosphatidic acid (LPA) is among the lipids that have recently been identified as regulators of the function of ion channels through direct or indirect actions. LPA is a phospholipid with biological activities that include platelet aggregation (Schumacher et al., 1979), cell proliferation, differentiation, and migration (Sheng et al., 2015) and has been linked to pathologies such as breast, prostate, and pancreatic cancers (Yamada et al., 2004; Liu et al., 2009) as well as to neuropathic pain (Inoue et al., 2004). Its activities are known to be mediated by at least six known G protein–coupled receptors, named LPA_{1-6} (Yung et al., 2014). LPA contains a glycerol backbone, a free phosphate group in position sn-3, and one fatty acid chain of varying length in either positions sn-1 or sn-2 that can be saturated or unsaturated. This gives rise to the different species of LPA, which have varied affinities for LPA receptors (van Corven et al., 1989).

Interestingly, LPA can interact with other types of proteins such as gelsolin and villin and shares the same binding site with PIP2, another negatively charged phospholipid, in each of these proteins (Goetzl et al., 2000; Kumar et al., 2004).

In recent years, there has been growing evidence that LPA directly modulates the activity of ion channels. Examples include members of the two-pore domain potassium channel family (Chemin et al., 2005), voltage-gated ion channels (Stirling et al., 2009), ligand-gated ion channels (Jans et al., 2013), and transient receptor potential (TRP) ion channels (Chemin et al., 2005; Nieto-Posadas et al., 2012; Kittaka et al., 2017).

For several years, LPA was thought to produce pain solely through the activation of specific G protein–coupled receptors. Recently, our group described that LPA can effectively activate the TRPV1 channel when applied to either the intracellular or extracellular faces of the membrane and that the response to LPA is dose dependent. Moreover, using a combination of biochemical and electrophysiological approaches, we also showed that LPA relies on at least one positively charged residue (K710) in the proximal C terminus of the TRPV1 channel to directly gate TRPV1. This activation by LPA is physiologically relevant since it

[1]Departamento de Neurociencia Cognitiva, División Neurociencias, Instituto de Fisiología Celular, Universidad Nacional Autónoma de México, México City, México;   [2]Departamento de Fisiología, Facultad de Medicina, Universidad Nacional Autónoma de México, México City, México.

*J.A. Canul-Sánchez and I. Hernández-Araiza contributed equally to this paper;   Correspondence to Tamara Rosenbaum: trosenba@ifc.unam.mx; León D. Islas: leon.islas@gmail.com.

leads to the generation of action potentials in dorsal root ganglia neurons and to pain in mice (Nieto-Posadas et al., 2012).

By further examining the effects of LPA on TRPV1-mediated currents, in this study we observed that LPA promotes an increase in the amplitude of macroscopic and single-channel currents, as compared with capsaicin. Changes in the surface charge or/and changes in the membrane properties caused by the insertion of negatively charged LPA molecules as well as a change in the permeability of the ion channel are mechanisms that could explain such an increase in the magnitude of TRPV1-mediated currents in response to LPA. Moreover, recent studies have proposed that the pore of TRPV1 and other TRP channels is dynamic and flexible, and it can adopt different conformational states in the presence of different ligands TRPV1 (Cao et al., 2013). Thus, in the present study we explored all of these possibilities in order to try to pinpoint the mechanism by which LPA produces an increase in the unitary conductance of the TRPV1 channel.

Materials and methods

Cell culture and transfection
The HEK293 cells (American Type Culture Collection; CRRL-11268) were maintained in standard cell culture conditions (37°C, 5% CO_2) in supplemented Dulbecco's modified Eagle's medium (DMEM; Gibco) with high glucose and complemented with 10% FBS (HyClone) and 100 U/ml of penicillin-streptomycin (Gibco). Cells were tested for mycoplasma and found free of infection (ATCC; 30-1012K). Cells were subcultured every 3 d using 0.05% (wt/vol) trypsin-EDTA solution and plated in coverslips pretreated with poly-D-lysine. Cells were cotransfected one day later with the pcDNA3.1 plasmid with WT rTRPV1 or rTRPV1-K710D and pIRES-GFP plasmids using JetPei (Polyplus transfection), according to manufacturers' instructions.

Site-directed mutagenesis
Point mutations in rTRPV1-pCDNA3.1 were made by a two-step PCR as previously described (Rosenbaum and Gordon, 2002).

Solutions
Stock solution of capsaicin (Sigma-Aldrich) was prepared at 10 mM in ethanol, and stock solutions of 1-bromo-3-(S)-hydroxy-4-(palmitoyloxy)butyl phosphonate (BrP-LPA; Echelon Biosciences; part L-7416) at 1 mM and tetrapentylammonium (TPA; Sigma-Aldrich; part 258962) at 200 mM were prepared in deionized water. Lysophosphatidic acid 18:1 (Avanti Polar Lipids; part 857130), LPA 18:0 (Avanti Polar Lipids; part 857128), and lysophosphatidylcholine 18:1 (LPC; Sigma-Aldrich; part L-1881) stocks were prepared at a concentration of 10 mM by dissolving the lipids in DMEM with 1% BSA. Stocks for LPA and LPC were vortexed 10 min, incubated 1 h at 37°C, and sonicated with a Branson 1510 bath ultrasonicator at 40 KHz for 15 min before being aliquoted and frozen in liquid nitrogen and stored at –70°C. Before using the aliquots for electrophysiological experiments, these were vortexed to thaw and incubated at 37°C for 20 min. The reagents were diluted to the desired concentration in recording solution.

Electrophysiological recordings
Currents were obtained from excised membrane patches in the inside-out patch clamp configuration, in isometric recording solutions containing 130 mM NaCl, 3 mM HEPES, and 1 mM EDTA (Sigma-Aldrich) adjusted to pH 7.2, unless otherwise stated. The borosilicate pipettes used had an average resistance of 5 MΩ for macroscopic currents and 10 MΩ for single-channel recordings. Currents were recorded using an EPC10-USB amplifier (HEKA Elektronic), filtered at 2 kHz (low-pass Bessel filter) and sampled at 10 kHz for macroscopic currents and filtered at 3 kHz and sampled at 50 kHz for microscopic currents. Data were acquired using either Pulse or Patchmaster software (HEKA Elektronic) and analyzed in Igor Pro (Wavemetrics Inc.). Solutions were changed using an RSC-200 rapid changer (Biological).

For macroscopic currents, the voltage protocol consisted of a holding potential of 0 mV for 10 ms followed by a square pulse to –60 and then another to +60 mV for 100 ms each and back to 0 mV for 10 ms. For every membrane patch, first we recorded the current in the absence of agonist in order to account for the leak current, then we recorded the current elicited by 4 µM capsaicin (a saturating concentration). After the membrane patch was washed with recording solution (until the seal resistance was close to values before capsaicin exposure), it was exposed to a saturating concentration of LPA (5 µM; EC_{50} is 754 nM; Nieto-Posadas et al., 2012), and the current elicited by LPA was normalized to that elicited by capsaicin. Mean current values for LPA were measured after channel activation had reached the steady state (∼3–5 min).

We measured the voltage dependence of the entry rate of the blocker TPA to the pore of the channels, as previously described (Jara-Oseguera et al., 2008). For these experiments, the patches were exposed first to 4 µM capsaicin or 5 µM LPA, washed, and reexposed to the agonists concomitantly with 20 µM TPA. After washing off the ligand, just before the beginning of each experiment with blocker, we obtained three leak traces, which were averaged to reduce noise. This leak average was subtracted from the experimental traces.

Currents were recorded in response to square voltage pulses where the voltage was held at 0 mV for 10 ms, then stepped from 40 to 140 mV in 20-mV intervals for 100 ms and then returned to 0 mV for 10 ms. For every voltage used, three current traces were averaged in the presence of the blocker and fitted to a simple exponential to obtain the block rate ($s^{-1} M^{-1}$). The voltage dependence of the blocking reaction was calculated by plotting the block rate (k_b) versus voltage and by fitting the data to the following function:

$$k_b = k_b(0) \cdot \exp\left(\frac{-Z_{app}V}{KT}\right), \tag{1}$$

where $k_b(0)$ is the rate constant at 0 mV, Z_{app} is the apparent charge associated with the blocking reaction, K is the Boltzmann constant, T is the temperature (298°K), and V is the voltage applied. To calculate the magnitude of the expected effect of surface charge, the surface potential was calculated from the Grahame equation for one electrolyte (Latorre et al., 1992):

$$\phi_s = (2RT/z_iF)\,ln\left[X + \sqrt[2]{(X^2 + 1)}\right], \tag{2}$$

where $X = \sqrt{136\sigma/C_i}$; σ is the surface charge; z_i is the charge of the main electrolyte (Na$^+$); C_i is the concentration of the main ions (NaCl); R is the gas constant, T is the absolute temperature in Kelvin, and F is Faraday's constant.

To determine whether LPA produced a change in the permeability of TRPV1 channels in response to activation by LPA, we measured the bi-ionic reversal potential (E_{rev}) between Na$^+$ and the organic monovalent cation, NMDG ($\sim$4.54 Å) when channels were activated with capsaicin or LPA. In these experiments, the pipette (extracellular solution) contained (in mM) 10 NaCl, 3 HEPES, 1 EDTA, and 120 NMDG. For the bath (intracellular solution), we used (in mM) 130 NaCl, 3 HEPES, and 1 EDTA; both solutions were adjusted to pH 7.4. The liquid junction potential (LJP) was corrected by measuring voltage in the current clamp mode in symmetric solutions and then again in asymmetrical solutions; the difference between the two voltages is the LJP. The typical LJP for NMDG solutions was 3.9 mV. The E_{rev} value from three voltage ramps (–120–120 mV, 1 V/s) from inside-out membrane patches was averaged, and the leak and LJP were subtracted before calculating the relative permeability with the Goldman–Hodgkin–Katz (Hille, 1971) equation:

$$E_{rev} = \frac{RT}{zF}\ln\left(\frac{[Na^+]_o P_{Na} + [X^+]_o P_x}{[Na^+]_i P_{Na} + [X^+]_i P_x}\right), \tag{3}$$

where R is the gas constant, E_{rev} is the reversal potential, F is the Faraday constant, T is absolute temperature (room temperature, 298°K), and $[X^+]$ is the concentration of ion X$^+$. Note that the extracellular solution contained 10 mM Na$^+$, which is necessary to maintain normal gating of TRPV1 (Jara-Oseguera et al., 2016).

For single-channel recordings, the borosilicate pipettes were covered with wax to reduce stray capacitance. To obtain the single-channel current amplitude in response to different agonists, the voltage protocol consisted of a series of 60-mV rectangular pulses lasting 1 s, with a holding potential of 0 mV for 10 ms. Once we obtained an inside-out membrane patch with only one TRPV1 channel, it was exposed to 4 µM capsaicin, then it was washed with recording solution until no openings were observed, and then it was exposed to one of the following conditions: (a) capsaicin + 0.0005% BSA in DMEM, as a control for the vehicle used for LPA; (b) LPA 5 µM; (c) BrP-LPA 5 µM, which is an LPA analogue we had previously reported as a TRPV1 activator (Nieto-Posadas et al., 2012); or (d) LPC 2.5 µM + 4 µM capsaicin, because LPC is a lipid with a geometry similar to LPA (Sprong et al., 2001; Biswas et al., 2007) but is not a TRPV1 agonist.

To obtain current–voltage curves for a single channel, we used inside-out membrane patches containing a single TRPV1 channel and exposed it to either 4 µM capsaicin or 5 µM LPA. To construct the current–voltage curve, we applied 500-ms pulses from –100 to +100 mV in 40-mV steps; the voltage was held at 0 mV during 5 ms before and after each pulse. For the analysis, 5–10 traces in which openings and closings were clearly observed were used to build all-points histograms after accounting for the leak current. The histograms were fitted to a Gaussian function where the peak corresponded with the unitary channel current amplitude. The presented current–voltage curves represent the average of three independent experiments.

Single-channel kinetics

Half-amplitude threshold crossing analysis (Colquhoun and Sigworth, 1985) was used to idealize single-channel recordings for kinetic analysis using custom-written programs in IgorPro software (Wavemetrics Inc.). Open and closed dwell times are presented as histograms according to the Sine–Sigworth transform (Sigworth and Sine, 1987). The filter dead time is calculated as $T_d = 0.179/f_c$. At f_c = 3 kHz, T_d = 63 µs. Events shorter than 100 µs were discarded. Open and closed time histograms were fit to sums of exponential components to extract time constants from the distributions. The burst length was calculated for bursts of openings, which are defined as groups of openings separated by closures shorter than a critical time T_{crit}. The value of T_{crit} was calculated by solving

$$e^{-t_{crit}/\tau_f} = 1 - e^{-t_{crit}/\tau_s}, \tag{4}$$

where τ_f and τ_s are the time constant of the fast and slow components of the closed time histograms, respectively. The open probability (P_o) was calculated for each sweep from idealized data, as the sum of the total open time divided by the sweep duration.

Statistical analysis

The data were subjected to Student's t test; $P < 0.05$ was considered statistically significant. Data are presented as mean ± SEM.

Results

Effects of LPA on TRPV1 unitary currents

As previously reported, TRPV1 is directly activated by LPA (Nieto-Posadas et al., 2012). Because of the fact that experiments with lysolipids are technically difficult, since the amphipathic character of these molecules affects membrane stability, we initially interpreted the increased currents with LPA as membrane patch instability. It was not until we performed experiments blocking the macroscopic currents in response to LPA and single-channel recordings that we were effectively able to discern that there is an increase in the magnitude of these currents that was not caused by disruption in the integrity of the membrane patches. We can now assert that indeed, LPA induces currents with a larger magnitude than those elicited by capsaicin. This is demonstrated in Fig. 1 A, which shows TRPV1 currents in the same patch, elicited by a square voltage pulse to –60 mV followed by a pulse to 60 mV, in the presence of either capsaicin or LPA. The average macroscopic currents of eight independent experiments with LPA (5 µM) was 1.36 ± 0.1–fold larger at –60 mV (P < 0.01) and 1.36 ± 0.056–fold larger at +60 mV (P < 0.01) compared with normalized currents elicited by capsaicin (4 µM; Fig. 1, B and C). In general, the macroscopic current (I) depends on the number of channels (N), which is unlikely to change substantially during inside-out recordings; on the open probability (P_o); and on the unitary current (i). We performed single-channel recordings to see which parameter was changing. In our experiments, the average single-channel current at 60 mV when TRPV1 is activated by capsaicin is 6.84 ± 0.2 pA.

Because the LPA stock was prepared in DMEM with 1% BSA, we also measured unitary currents activated with capsaicin + 0.0005% BSA, which is the same final amount of BSA in ex-
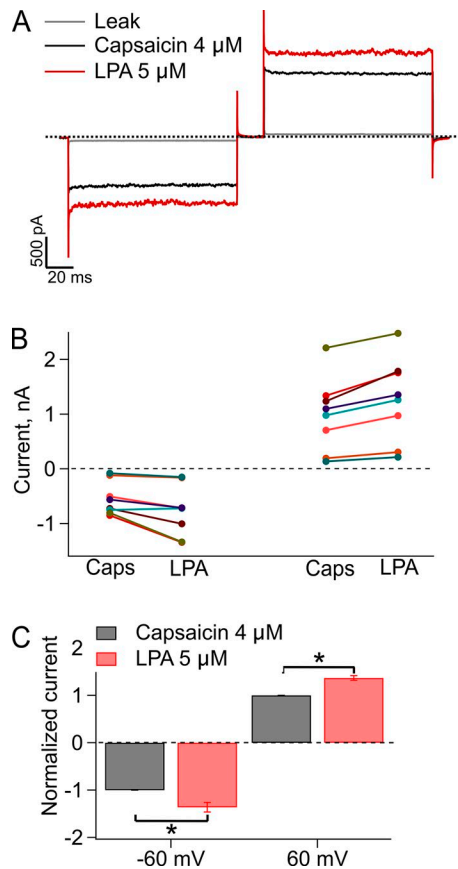
Canul-Sánchez et al.
Different agonists promote distinct TRPV1 open states

Journal of General Physiology
https://doi.org/10.1085/jgp.201812141

1737

Figure 1. **Macroscopic currents in WT TRPV1 activated by 4 µM capsaicin or 5 µM LPA. (A)** Representative currents at –60 and +60 mV. The gray lines correspond to the leak current, the black lines are the response to capsaicin, and the red lines are the response to LPA. The dashed line indicates zero current. **(B)** Paired data for eight independent experiments at –60 and at 60 mV. Each color represents one membrane patch. **(C)** The bar graph corresponds to the normalized currents of data in (B). Data obtained in the presence of LPA 5 µM are normalized to the current elicited by 4 µM capsaicin, where values for currents elicited by the latter agonist were set to 1 (gray bars). The increase elicited by LPA was 1.36 ± 0.1–fold larger at –60 mV (*, P < 0.01, n = 8) and 1.36 ± 0.056–fold larger at +60 mV (*, P < 0.01, n = 8), as compared with capsaicin. Recordings were performed in the inside-out configuration of the patch clamp, the holding potential was 0 mV, and 60 and –60 mV square pulses lasted 100 ms. Leak currents were obtained first; then capsaicin was applied to obtain the currents elicited by this agonist; then capsaicin was washed; and finally, currents in the presence of LPA were obtained. Agonists were applied using a rapid solution changer, as described in the Materials and methods section. Group data are reported as the average ± SEM.
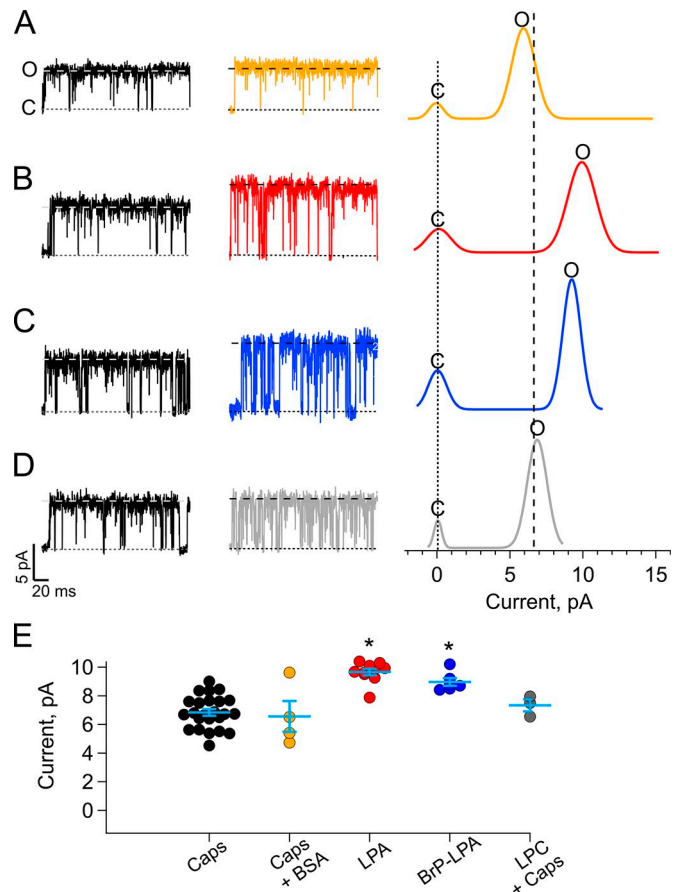

Figure 2. **LPA produces an increase in single-channel currents in TRPV1 channels heterologously expressed in HEK293. (A–D)** Representative traces from single-channel recordings of TRPV1 channels in the inside-out configuration, as compared with capsaicin. The letters c and o represent the closed and open state levels shown in the histograms. The vertical dotted lines represent the average single-current amplitude elicited by capsaicin (6.84 ± 0.23 pA; n = 24) before the application of treatment. **(A)** Capsaicin 4 µM + BSA 0.0005% (6.57 ± 1 pA; n = 4). **(B)** LPA 5 µM in BSA 0.0005% (9.66 ± 0.23 pA; n = 10). **(C)** BrP-LPA 5 µM (8.97 ± 0.27 pA; n = 6). **(D)** Capsaicin 5 µM + 2.5 µM LPC (7.34 ± 0.41 pA; n = 3). **(E)** Summary of the results in A–D. Lines between the symbols indicate average ± SEM. *, statistical significance P < 0.01. The fold increase in current amplitude in each case is as follows: capsaicin + BSA, 0.96 ±0.16; LPA 5 µM, 1.41 ± 0.03; BrP-LPA 5 µM, 1.31 ± 0.04; and LPC 2.5 µM + capsaicin 4 µM, 1.07 ± 0.05. Recordings were made applying a series of 1-s-long, 60-mV square pulses from a 0-mV holding potential; data were sampled at 50 kHz and filtered with at 3-kHz low-pass Bessel filter. Each seal was exposed to 4 µM capsaicin, washed, and then exposed to the indicated lipid by perfusion using a rapid solution changer.

periments with phospholipids. For these experiments, we alternated treatments by applying only capsaicin (representative black traces, Fig. 2, left), washing with recording solution, and then adding the agonist (color traces, Fig. 2, middle). As shown in Fig. 2, A and E, no increase in the current amplitude was found under these conditions (6.57 ± 1.08 pA with capsaicin + 0.0005% BSA [yellow trace] vs. 6.84 ± 0.2 pA [black trace; P > 0.01] for capsaicin alone). Remarkably, 5 µM LPA elicited a statistically significant increase in TRPV1 unitary current (Fig. 2, B and E; 9.66 ± 0.22 pA vs. 6.84 ± 0.23 pA for capsaicin; P < 0.01). 1-bromo-3-(S)-hydroxy-4-(palmitoyloxy) butyl phosphonate (BrP-LPA; 5 µM), which activates TRPV1 by binding to the same residue in the C terminus as LPA does (Nieto-Posadas et al., 2012),

also produced an increase in unitary current amplitude, albeit smaller than that observed with LPA (Fig. 2, C and E; 8.97 ± 0.27 pA vs. 6.84 ± 0.23 pA for capsaicin; P < 0.01).

LPA and BrP-LPA are phospholipids than can get inserted in the cell membrane and might change its mechanical properties and/or shape. Therefore, we tested the effect of LPC, which has been shown to produce changes in the curvature of membranes (Lundbaek and Andersen, 1994). Because we had reported that this phospholipid does not activate TRPV1 (Morales-Lázaro et al., 2014), LPC was coappled with capsaicin (4 µM capsaicin + 2.5 µM LPC). These experiments show no significant changes in the unitary current (Fig. 2, D and E; 7.34 ± 0.41 vs. 6.84 ± 0.23
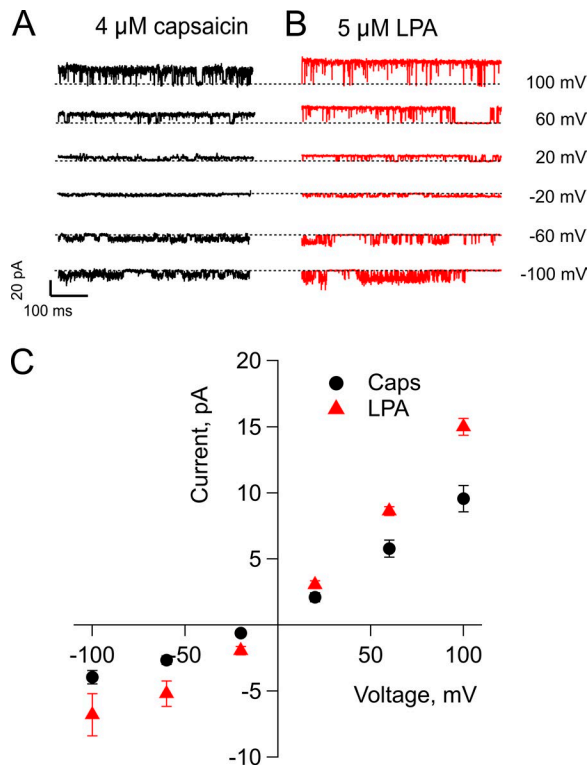
Figure 3. **LPA induces an increase in current at both positive and negative potentials. (A and B)** Representative traces for the currents elicited by 4 µM capsaicin (A) or by 5 µM LPA (B) at different potentials. The dashed line indicates zero-current level. **(C)** Summary of the microscopic current–voltage relations for capsaicin-elicited currents (black circles) and LPA-elicited currents (red triangles). Data are presented as mean ± SEM., n = 5. The increase in current is significant P < 0.05 at –100, –60, –20, 60, and 100 mV (Student's t test). Single-channel recordings were performed in the inside-out configuration of the patch clamp, with a holding potential of 0 mV and increasing square voltage pulses as indicated.

for capsaicin alone; P > 0.01) when channels were exposed to LPC and capsaicin.

These experiments support the hypothesis that LPA produces its effects on single-channel current amplitude through a mechanism that probably does not involve changes in membrane physical properties.

The effects of LPA on single-channel current amplitude discussed above (Fig. 2, B and E) were evaluated at a voltage of +60 mV. We next wondered whether this effect was present when TRPV1 channels were activated with LPA and challenged at different voltages. Thus, we compared the single-channel amplitudes of current–voltage relationships for TRPV1 activation by capsaicin or LPA. The data in Fig. 3, A–C, show that at all the voltages tested (–100 to 100 mV), the unitary currents produced by LPA activation were larger than the ones produced by capsaicin, indicating that the LPA effect is not voltage dependent.

Gating of channels by LPA and capsaicin
At saturating concentrations of capsaicin (4 µM) or LPA (5 µM), channels gate in a very similar way (Fig. 4, A–D). The P_o values are 0.81 ± 0.02 (n = 3) and 0.78 ± 0.04 (n = 3) in capsaicin and LPA, respectively, and do not exhibit significant differences (P >

0.01) but indicate that LPA is a full agonist of TRPV1. The burst length distribution has at least three components, indicating a complex gating mechanism. The LPA-activated channels show a slight preponderance of longer bursts (Fig. 4, C and D). At subsaturating concentrations of both capsaicin (50 nM) and LPA (1 µM), the gating behavior is again complex (Fig. 4, E–H). Burst length is diminished, such that individual bursts can be clearly discerned (Fig. 4, F and H). Three types of bursts are present in the distributions, with LPA again showing a higher proportion of longer and intermediate bursts (see Table 1 for values). The values of all the fit parameters are collected in Table 1.

The multiexponential nature of the burst duration histograms indicates the presence of multiple open and closed states and is characteristic of allosteric gating (Hui et al., 2003; Liu et al., 2003; Latorre et al., 2007; Baez et al., 2014). Interestingly, the data indicate that all open states with LPA have the same conductance and that this phospholipid increases the conductance of all open states as well. LPA also seems to favor longer bursts at both subsaturating and saturating concentrations.

A change in membrane surface charge does not account for the effects of LPA on TRPV1-mediated currents
Up to this point, the data show that LPA produces an increase in the single-channel conductance, as compared with capsaicin. Also LPA seems to dissociate more slowly from its binding site as indicated by an increased burst length. A possible mechanism for the increase in single-channel conductance is that because LPA has a negatively charged polar head and can be inserted into the membrane, increasing the surface charge and generating a negative surface potential might increase the local concentration of permeant ions at the intracellular pore entrance, as predicted by the Gouy–Chapmann–Stern theory (Oldham, 2008).

Assessing the role of increased surface charge on the conductance and gating of several ion channels has been achieved in part thanks to a strategy that involves the use of divalent or multivalent ions at high (mM) concentrations to screen the surface charge (Hille et al., 1975). However, this is not an option when studying TRPV1, because it has been extensively described that divalent (i.e., Ca^{2+}) and multivalent ions produce block or desensitization of the channel (Koplas et al., 1997; Ahern et al., 2005; Mergler et al., 2011; Samways and Egan, 2011). Thus, to determine the role of an increase in surface charge by LPA, we used a strategy based on applying pore blockers whose actions are voltage dependent. If the increase in conductance is simply caused by LPA producing a local negative potential and thus increasing the local concentration of Na^+ near the pore entrance, one should expect that this surface potential will also increase the rate of channel block by a positively charged pore blocker (Park et al., 2003; Jara-Oseguera et al., 2008). Thus, to test for this possibility, we used TPA block as a probe of the local surface charge, as has been reported previously (Thompson and Begenisich, 2000; Oseguera et al., 2007; Jara-Oseguera et al., 2008). Fig. 5 A shows representative macroscopic currents obtained at different voltages in the presence of 20 µM intracellular TPA and 4 µM capsaicin (Fig. 5 A, top) or 5 µM LPA (Fig. 5 A, bottom), as well as in the average relationship between the voltage and the blocking rate (Fig. 5 B). Although it is evident that the block rate is voltage dependent,
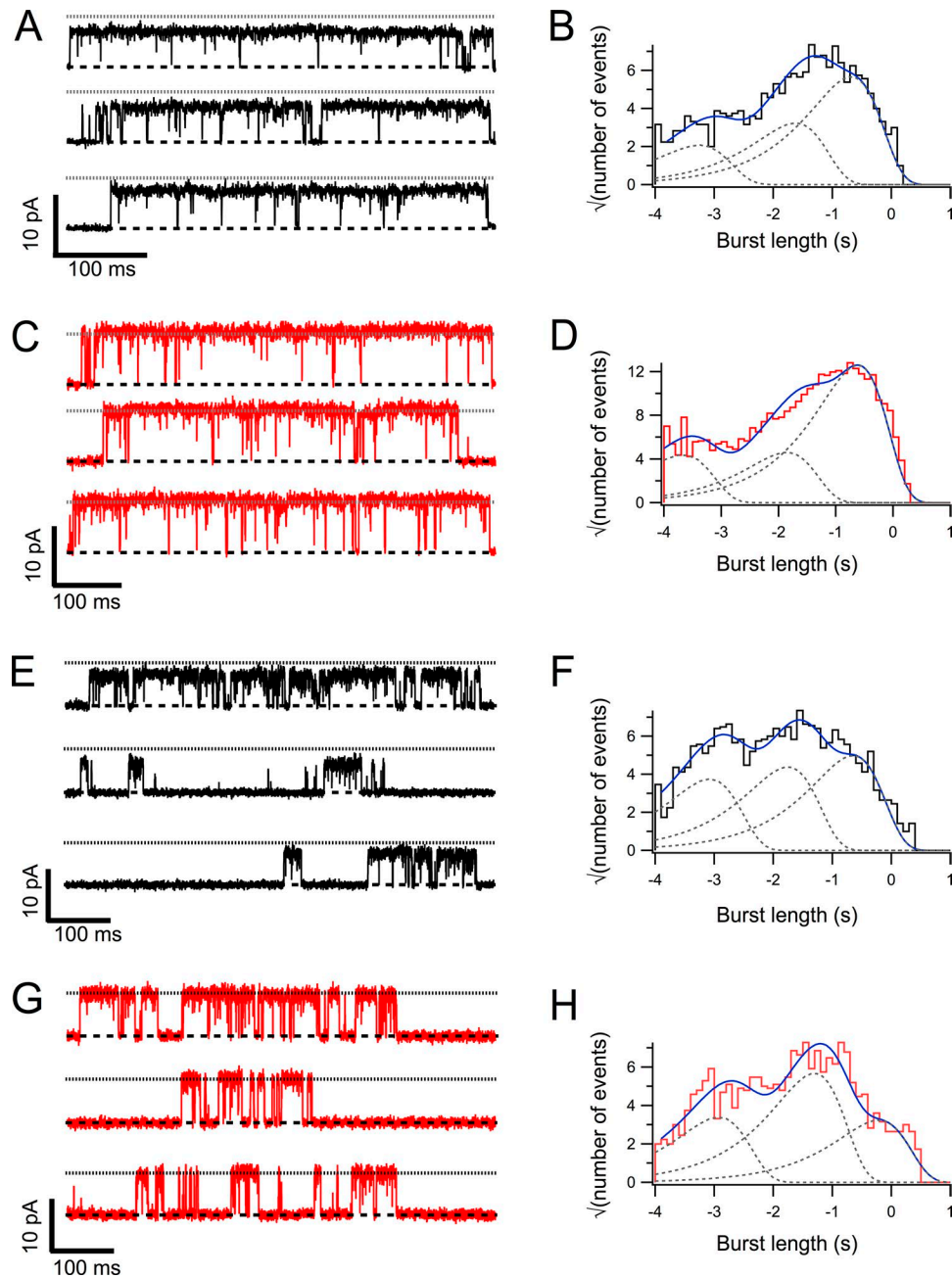
Figure 4. **Single-channel gating of TRPV1 channels with capsaicin or LPA. (A)** Representative segments of single-channel records in the presence of capsaicin 4 µM. The dashed and dotted lines represent the zero-current level and the current level when the same channel is opened by LPA, respectively. **(B)** Burst length distribution. The continuous line on top of the histogram is the fit to a sum of three exponentials, which are shown individually by the gray dotted lines. **(C)** A single TRPV1 channel opened by LPA 5 µM. Representative openings with the dashed and dotted lines indicating zero-current and open current levels, respectively. **(D)** Burst length distribution. The continuous line on top of the histogram is the fit to a sum of three exponentials, which are shown individually by the gray dotted lines. **(E)** Representative segments of a single-channel recording with subsaturating 50 nM capsaicin. Lines have the same meaning as in A. **(F)** Burst length distribution. The continuous line on top of the histogram is the fit to a sum of three exponentials, which are shown individually by the gray dotted lines. **(G)** Recordings from a single channel activated by 1 µM LPA. The lines indicate current levels as in C. **(H)** Burst length distribution. The continuous line on top of the histogram is the fit to a sum of three exponentials, which are shown individually by the gray dotted lines. The parameters of the exponential fits are compiled in Table 1. Recordings were made applying up to 100 3-s-long, 60-mV square pulses from a 0-mV holding potential; data were sampled at 50 kHz and filtered with a 3-kHz low-pass Bessel filter. Capsaicin and LPA were applied by perfusion with a rapid solution changer.

the voltage dependence of blockade is not different for capsaicin and LPA, as the $K_b(0)$ (Eq. 1) are $1.10^6 \pm 4.6\,10^5\,s^{-1}\,M^{-1}$ for capsaicin and $1.32 \times 10^6 \pm 3.5 \times 10^5\,s^{-1}\,M^{-1}$ for LPA activation. The apparent charge associated with blocking of the channel is 0.43 ± 0.08 for capsaicin and 0.34 ± 0.05 for LPA.

What is the expected effect of an increased negative surface charge on the TPA blocking rate? The partition coefficient, K, of LPA in the lipid membrane is not known, but we can use the value of $K = 12 \times 10^3\,M^{-1}$ for a similar lysophospholipid, LPC16, as an approximation (Henriksen et al., 2010). With this value, a
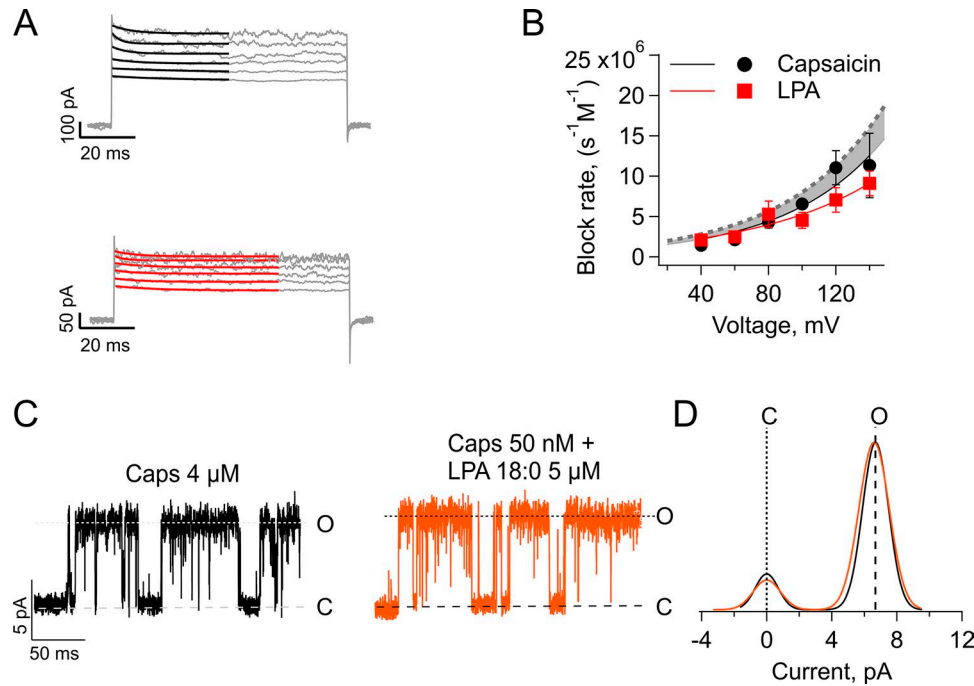
Figure 5. **Estimation of the effect of surface charge on the kinetics of block by TPA and single-channel conductance. (A)** The TPA (20 µM) block kinetics with 4 µM capsaicin (top) or 5 µM LPA (bottom). The superimposed black and red lines represent the exponential fits. **(B)** Voltage dependence of block for currents elicited by capsaicin (circles, solid fit, $n = 4$) or LPA (squares, dashed fit, $n = 8$). Data are plotted as mean ± SEM. From the exponential fit we obtained the following parameters: $k_b(0) = 1.10^6 \pm 4.6\ 10^5\ s^{-1}\ M^{-1}$ for capsaicin, and $k_b(0) = 1.32 \times 10^6 \pm 3.5\ 10^5\ s^{-1}\ M^{-1}$ for LPA (P > 0.01), while $Z_{app} = 0.43 \pm 0.08$ for capsaicin, and $Z_{app} = 0.34 \pm 0.05$ for LPA (P > 0.01). The dashed curve is the increase in the blocking rate expected if LPA contributes −14 mV of surface potential, as calculated in the text. This shows that the blocker entrance to the pore is electrostatically shielded from the membrane surface potential. **(C)** Representative traces from single-channel recordings of TRPV1 channels in the inside-out configuration at +60 mV, in response to 4 µM capsaicin (black) or 50 nM capsaicin + 5 µM LPA 18:0 (orange). **(D)** Comparison of the single-current amplitude elicited by capsaicin alone (black) or in combination with LPA 18:0 (orange) for experiment shown in (C). The mean single-current amplitude elicited for four independent experiments was 7.33 ± 0.21 pA for capsaicin 4 µM and 7.27 ± 0.17 pA for capsaicin in combination with LPA 18:0 (P > 0.01). Macroscopic current recordings were performed in the inside-out configuration of the patch clamp, the holding potential was 0 mV, and 100-ms-long square pulses from 40 to 140 mV (in 20-mV increments) were applied.

per lipid area of 70 Å², and a typical patch area of ~12 × 10⁸ Å², we can calculate the expected number of LPA molecules partitioned into the membrane in our inside-out patches to be ~10⁶. This gives an expected surface charge density of ~80 × 10⁻⁵ e₀/Å². Using the Grahame equation with our ionic conditions (Grahame, 1947), this surface charge should produce an equivalent surface potential of approximately −15 mV. In Fig. 5 B, we plot the expected increase of the blocking rate (gray dotted line). It can be seen that if LPA has any effect in blocking rate, it is to diminish it at positive voltages.

In addition, we tested whether LPA 18:0, which does not activate TRPV1 but has the same amount of charge as LPA18:1 does, increased single-channel current amplitudes when coapplied with 50 nM capsaicin. Fig. 5, C and D, show that LPC 18:0 does not affect the conductance of the channel. These data and analyses suggest that LPA does not produce a change in the electric potential in the vicinity of the inner pore of TRPV1, thus ruling out a change in membrane surface charge as a cause for the increased conductance we observe with LPA.

Table 1.   **Fit parameters for single-channel kinetic analysis**

Condition	Burst duration fits					
	A₁	Tau₁[a]	A₂	Tau₂	A₃	Tau₃
Saturating agonist						
Capsaicin 4 µM	3.42	0.556	5.32	23.81	9.34	207.83
LPA 1 µM	7.23	0.215	7.57	13.81	20.75	239.69
Subsaturating agonist						
Capsaicin 50 nM	6.19	0.841	7.23	17.61	8.20	222.35
LPA 1 µM	5.60	1.189	9.34	49.56	5.33	604.9

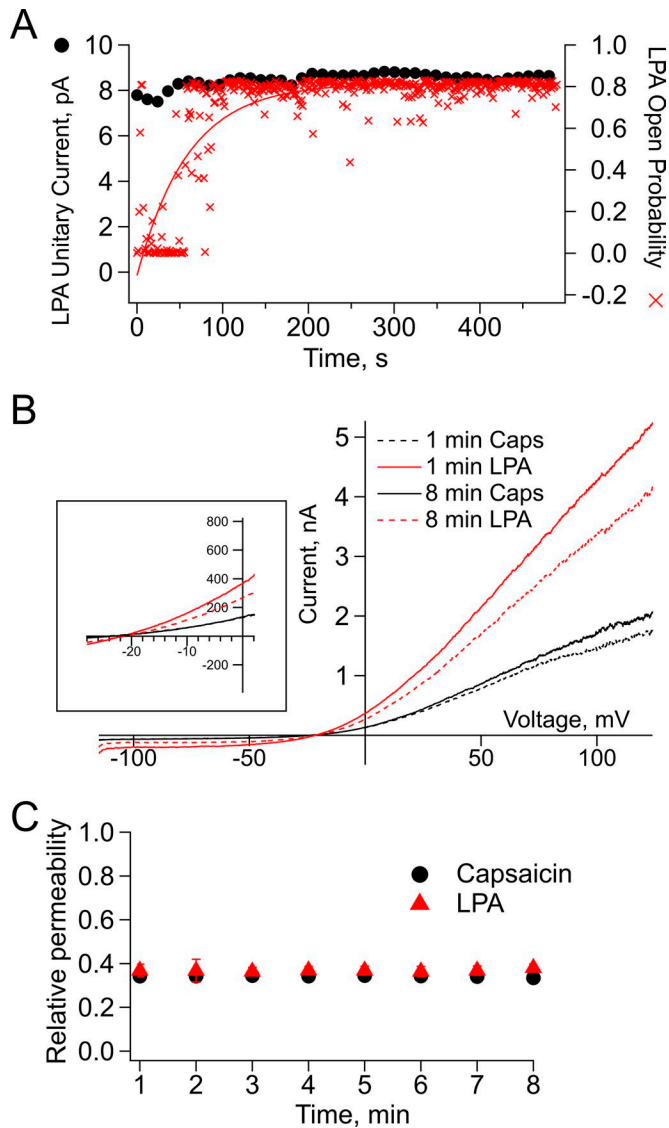[a]Time constant units (Tau) are in milliseconds.

Figure 6. **Relative permeability for large organic cations with respect to sodium. (A)** Unitary current amplitudes (black circles) and open probability (red crosses) of TRPV1 in response to LPA relative to time. While the unitary current remains stable over time, the open probability increases with time until reaching a maximum after 3 min. **(B)** Representative traces elicited by voltage ramps (–120 to 120 mV) from inside-out membrane patches exposed to capsaicin (4 µM) for 1 min (solid black) and for 8 min (dashed black) and to LPA (5 µM) for 1 min (solid red) and 8 min (dashed red). The right graph zooms in the region of the curves where the E_{rev} occurs for all four conditions stated above. **(C)** Relative permeability of NMDG (~4.5A°) in response to capsaicin (black; $n = 3$) or LPA (red; $n = 10$). Lines between the symbols indicate mean ± SEM. No statistical differences among permeabilities at the different times measured were found for this set of data; $P > 0.01$.

The increased conductance with LPA is instantaneous and is not accompanied by a large change in ion selectivity to large cations

To assess if the increase in TRPV1's single-channel conductance occurs immediately when the channel opens in the presence of LPA, we analyzed how the P_o in response to activation by LPA changed with time and compared it with the value of the single-channel current amplitude over a period of 500 s. LPA is a slower agonist of TRPV1 in comparison to capsaicin (Nieto-

Posadas et al., 2012), perhaps because it accesses its binding site from the lipid membrane. The P_o of each sweep of 1 s duration was calculated and plotted as a function of the number of each 500 sweeps. This analysis evidences the slow time course of increase in P_o in response to LPA (Fig. 6 A, red crosses). However, the single-channel current amplitude remains constant through time (Fig. 6 A, black circles). This means that even the first, low open probability openings in response to LPA have an increased conductance.

Next, to assess whether the increased conductance of TRPV1 with bound LPA is accompanied by a change in ion selectivity, we tested for changes in the permeability to NMDG (4.5 Å) relative to Na^+ when the channel is activated by LPA or capsaicin. Fig. 6 B shows representative traces of inside-out membrane patches elicited by voltage ramps when exposed to capsaicin (black) or LPA (red) for 1 (solid lines) or 8 min (dashed lines). Fig. 6 B, right, shows that the E_{rev} under each experimental condition in the presence of NMDG is not significantly shifted. Moreover, the experiments in Fig. 6 C show that when TRPV1 is activated with LPA, there is no increase in the permeability for the larger cation NMDG relative to Na^+ through time starting from 1 min of exposure to capsaicin or LPA (0.34 ± 0.009 with capsaicin vs. 0.36 ± 0.02 with LPA) up to 8 min of exposure to the agonists (0.33 ± 0.007 with capsaicin vs. 0.38 ± 0.02 with LPA). These results indicate that when TRPV1 is activated by LPA, there is a marked increase in conductance upon exposure to the ligand, but this is not accompanied by a change in selectivity, indicating that the integrity of the selectivity mechanism is conserved in both pore configurations.

Coactivation of TRPV1 with LPA and capsaicin

If the two ligands studied here are capable of stabilizing different pore conformations, it should be possible to observe these conformations independently in a single channel in a coapplication experiment. We found that the most favorable condition for this experiment was to keep both ligands at a subsaturating concentration. Fig. 7 A, left, shows the representative openings from a patch with a single channel to which 50 nM capsaicin, 50 nM capsaicin + 1 µM LPA, and 1 µM LPA were applied, in that order. Notice that in the presence of both ligands, two types of events are detected, low and high conductance, which correspond to the events detected with either capsaicin or LPA, respectively. The experiment is quantitated in Fig. 7 A, middle. The amplitude of each detected opening event is plotted as a function of that event duration. It can clearly be observed that in this experiment, the amplitude of capsaicin-evoked events is small (mean 8 pA ± 0.23), while the average amplitude of LPA-evoked events is 9.8 pA ± 0.31. In the presence of both ligands, the distribution shows two types of events corresponding to the amplitudes observed with capsaicin or LPA alone. This is also seen in the all-points histograms from selected opening events (Fig. 7 A, right). We made sure the patch contained a single channel by applying a saturating concentration of LPA at the end of the experiment and observing the absence of overlapping openings. This experiment clearly indicated that the same channel can be activated to different open conformations by two different full ligands.
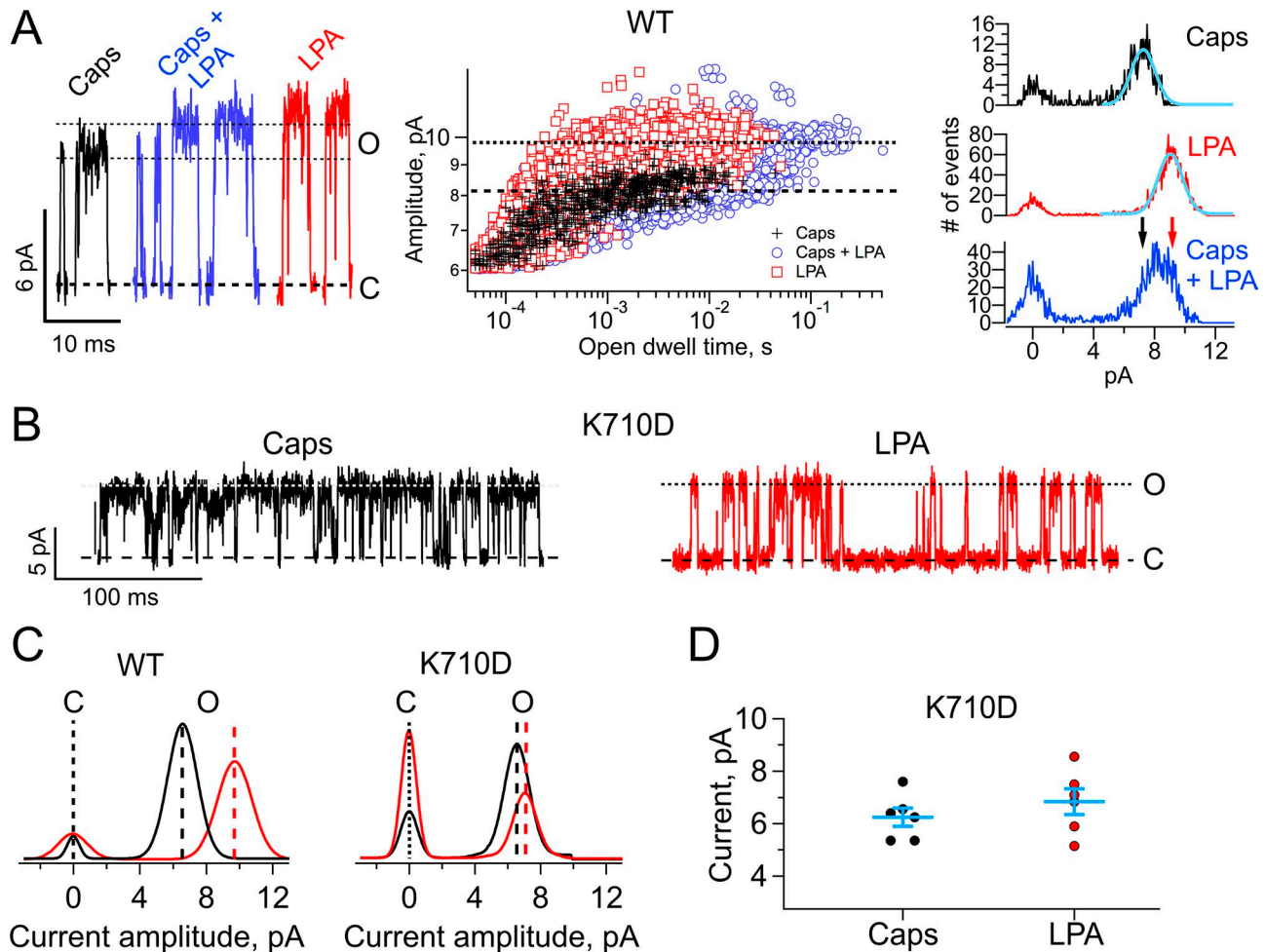
Canul-Sánchez et al.
Different agonists promote distinct TRPV1 open states

Journal of General Physiology
https://doi.org/10.1085/jgp.201812141

1742

Figure 7. **A single channel can be activated to two conductance states by coapplication of LPA and capsaicin. (A)** Left: Three classes of openings from the same single channel are observed. The low conductance and high conductance are prevalently observed with capsaicin or LPA, respectively. The two types are observed when capsaicin and LPA are applied together. Middle: To quantitatively evaluate the presence of the two levels of conductance, the amplitude of each detected event is plotted as a function of its duration. Capsaicin openings (black crosses) have mean amplitude of 8 pA; LPA openings (red squares) have amplitude of 9.8 pA. Openings elicited with capsaicin and LPA together show the presence of both types of openings (blue circles), with mean amplitudes 9.8 and 8.3. The membrane potential is 60 mV. Right: All-points histograms of selected openings in the three conditions. The histogram with LPA + cap is wider because of the presence of the two types of openings with two different amplitudes. Gaussian functions have been fitted to the histograms with capsaicin and LPA alone, as a visual guide. The arrows indicate the mean amplitudes of the openings with capsaicin (black) or LPA (red). **(B)** Representative traces of single-channel current elicited by capsaicin 4 µM (black) or 5 µM LPA (red) in the TRPV1 mutant K710D. **(C)** All-points histograms in the presence of capsaicin 4 µM (black) or 5 µM LPA (red) for TRPV1-WT (left) and for TRPV1-K710D (right). The value for single-channel current amplitude for TRPV1-WT in the presence of capsaicin 4 µM was 6.84 ± 0.02 pA (n = 24) and 9.66 ± 0.02 pA (n = 10) in the presence of 5 µM LPA. For TRPV1-K710D the single-channel current amplitude elicited by capsaicin 4 µM was 6.25 ± 0.4 pA (n = 6) and 6.84 ± 0.59 pA (n = 6) for LPA 5 µM. **(D)** Summary of the effects of LPA on the K710D mutant. Lines between the symbols indicate mean ± SEM. Recordings were made applying up to 100, 3-s-long, 60-mV square pulses from a 0-mV holding potential; data were sampled at 50 kHz and filtered with a 3-kHz low-pass Bessel filter. Capsaicin, LPA, and the combination of both agonists were applied by perfusion with a rapid solution changer.

LPA interacts with the K710 residue to promote changes in single-channel currents from TRPV1

So far we have shown that unspecific mechanisms (alteration of membrane physical properties and surface charge) are not responsible for the increased single-channel conductance elicited by LPA activation of TRPV1. This leaves a direct interaction of LPA with a binding site in TRPV1 (Nieto-Posadas et al., 2012) as a testable mechanism. To test this, we recorded single-channel currents from the charge-reversal mutant TRPV1-K710D in response to saturating concentrations of capsaicin or LPA (Fig. 7). Single-channel current amplitudes from TRPV1-K710D–expressing membrane patches were recorded at a voltage of 60 mV. As

shown in the representative recording (Fig. 7, B–D), the P_o for activation by LPA is reduced to 0.25 ± 0.03, as compared with that of the WT TRPV1 channel (0.78 ± 0.04, P < 0.01). Moreover, comparing the single-channel current amplitudes elicited by LPA in TRPV1-K710D and in the WT TRPV1 channel, we observed that there is a significant decrease in current amplitude in TRPV1-K710D (6.84 ± 0.59; Fig. 7, B–D) as compared with the WT TRPV1 (9.66 ± 0.02 pA, P < 0.01). As for capsaicin, no differences in single-channel current amplitude were observed between TRPV1-K710D (6.25 ± 0.4 pA) and WT TRPV1 (6.84 ± 0.2 pA; P > 0.01). These data are consistent with the interpretation that the change in single-channel current amplitude induced by

LPA is not caused by changes in the membrane physical properties produced by accumulation of LPA and that an increase in surface charge is not an underlying mechanism for this process. Because the concomitant addition of capsaicin and LPA elicits two different conducting states and the K710D mutant abolishes the increase in unitary conductance caused by LPA, we conclude that this phospholipid causes a different open conformation to that produced by capsaicin through a mechanism that requires the presence of K710.

Discussion

The TRPV1 is an ion channel that exhibits an exquisite array of responses to different stimuli, with its activity being regulated by molecules that act as agonists or by modulators that influence the gating properties of the channel (i.e., PIP_2; Ufret-Vincenty et al., 2011). LPA is a recently described agonist of TRPV1, which activates the channel through an interaction of this phospholipid with a positively charged amino acid in the C terminus, K710 (Nieto-Posadas et al., 2012). Here, we have studied the effects of LPA on TRPV1 currents in detail.

An interesting feature of this channel is that it may adopt different conformations in response to various agonists, as shown in recent cryo-EM studies where structures of TRPV1 were obtained in the presence of distinct agonists (Cao et al., 2013; Liao et al., 2013).

The results of the present study show that besides increasing the open probability, LPA produces changes in the single-channel conductance of TRPV1. When we examined the effects of LPA on single-channel currents, we found that the current amplitude was increased by 41 ± 0.08%, as compared with that produced by capsaicin. Another similar phospholipid, LPC, which does not activate TRPV1 but has been shown to affect gramicidin channel conductance by altering membrane–channel hydrophobic matching (Lundbaek and Andersen, 1994), does not change TRPV1 single-channel conductance when applied together with capsaicin, suggesting that the LPA effects are specific and not related to its effects on bilayer physical properties. We also find that in experiments in which capsaicin was coapplied together with LPA 18:0, a lipid that does not activate the TRPV1 channel (Morales-Lázaro et al., 2014), the single-channel currents do not exhibit an increase in the conductance.

Finally, our results using voltage dependence of the blocking rate by TPA as a reporter of the surface potential show that the inner pore is essentially shielded from any membrane surface charge contributed by LPA, ruling out an electrostatic mechanism for the increased conductance caused by LPA. Moreover, the fact that LPA increases single-channel current amplitude at negative and positive voltages, when applied to the intracellular side of TRPV1, is also consistent with the idea that its effects are not through a surface charge change mechanism because if this was the case, we would expect only the outward currents to be affected. Together, all of these data support our conclusion that LPA 18:1 produces an increase in the conductance of TRPV1 through a mechanism that is not dependent on the surface charge. It has been found that the increased conductance in BK channels observed in the presence of phospatidylserine is not caused by increased surface charge (Park et al., 2003).

How different are the open states induced by LPA and capsaicin? When we analyzed TRPV1 single-channel kinetics in the presence of either ligand, we found that LPA is a full agonist and that it promotes longer burst durations than capsaicin. It also indicates that both ligands promote occupancy of the open state by shifting gating to longer burst at higher agonist concentration. This suggests that the gating mechanism is similar for both ligands.

To assess the stability of the distinct open states induced by LPA and capsaicin, we measured the relative permeability to Na^+ and NMDG when the channel is opened by capsaicin or LPA. The results of these experiments show that (a) long-lived exposure to capsaicin in the presence of NMDG did not produce changes in the relative permeability to Na^+ in excised membrane patches and (b) exposure to LPA did not produce changes in the relative permeability to NMDG. These observations suggest the conclusion that although the rate of ion conduction is increased by LPA, the structure of the pore remains selective.

Cao et al. (2013) had determined that different conformational states can be achieved in TRPV1 when the channel is in the presence of agonists such as the vanillotoxin together with resiniferatoxin as compared with capsaicin. By coapplication of capsaicin and LPA we found that two different single-channel conductances could be distinguished: one that corresponded in amplitude to that attained with capsaicin and one that corresponded to the one elicited by LPA. This result indicates that the channel can distinctly open to two open states with distinct conductances. The different open states can be accessed when the channel is opened by different agonists (Scheme 1).
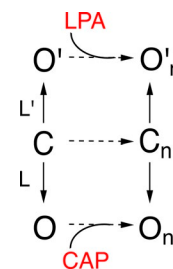
Simple allosteric model to explain the two conductance levels observed in TRPV1.

The channel can have an opening transition to two open states indicated by O_n and O'_n which have different single-channel conductance levels. Each agonist is capable of allosterically stabilizing each distinct set of open channels. The equilibrium constants L and L′ are shown as different because LPA promotes longer bursts than capsaicin.

Finally, we had previously reported that the Lys710 residue (Nieto-Posadas et al., 2012), located at the TRP box in the C-terminal domain, is part of the binding site for LPA (Nieto-Posadas et al., 2012; Cao et al., 2013). When this residue is mutated, the channel responds poorly to LPA, although we had previously discussed that there are probably other residues involved in the interaction with the channel (Nieto-Posadas et al., 2012). In our single-channel experiments with the K710D mutant, we observed

not only that there was a significant decrease in the P_o for activation by LPA but also that the single-current amplitude was no longer significantly increased when compared with capsaicin, further supporting our conclusion that LPA promotes an open state that is different to that supported by capsaicin.

In conclusion, we show that two different full agonists of TRPV1, LPA and capsaicin, produce activation of TRPV1 through an increase in the P_o of the channel that is accompanied by distinct single-channel conductance levels. This observation is congruent with recent structural work that suggests that the pore of TRP channels is dynamic and can adopt different conformations with different ligands.

Acknowledgments

References

Ahern, G.P., I.M. Brooks, R.L. Miyares, and X.B. Wang. 2005. Extracellular cations sensitize and gate capsaicin receptor TRPV1 modulating pain signaling. *J. Neurosci.* 25:5109–5116. https://doi.org/10.1523/JNEUROSCI.0237-05.2005

Baez, D., N. Raddatz, G. Ferreira, C. Gonzalez, and R. Latorre. 2014. Gating of thermally activated channels. *Curr. Top. Membr.* 74:51–87. https://doi.org/10.1016/B978-0-12-800181-3.00003-8

Biswas, S.C., S.B. Rananavare, and S.B. Hall. 2007. Differential effects of lysophosphatidylcholine on the adsorption of phospholipids to an air/water interface. *Biophys. J.* 92:493–501. https://doi.org/10.1529/biophysj.106.089623

Cao, E., M. Liao, Y. Cheng, and D. Julius. 2013. TRPV1 structures in distinct conformations reveal activation mechanisms. *Nature.* 504:113–118. https://doi.org/10.1038/nature12823

Chemin, J., A. Patel, F. Duprat, M. Zanzouri, M. Lazdunski, and E. Honoré. 2005. Lysophosphatidic acid-operated K+ channels. *J. Biol. Chem.* 280:4415–4421. https://doi.org/10.1074/jbc.M408246200

Colquhoun, D., and F.J. Sigworth. 1985. Single-Channel Recording. B. Sakmann, and E. Neher, editors. Plenum Press, New York, NY. 191–263.

Goetzl, E.J., H. Lee, T. Azuma, T.P. Stossel, C.W. Turck, and J.S. Karliner. 2000. Gelsolin binding and cellular presentation of lysophosphatidic acid. *J. Biol. Chem.* 275:14573–14578. https://doi.org/10.1074/jbc.275.19.14573

Grahame, D.C. 1947. The electrical double layer and the theory of electrocapillarity. *Chem. Rev.* 41:441–501. https://doi.org/10.1021/cr60130a002

Henriksen, J.R., T.L. Andresen, L.N. Feldborg, L. Duelund, and J.H. Ipsen. 2010. Understanding detergent effects on lipid membranes: A model study of lysolipids. *Biophys. J.* 98:2199–2205. https://doi.org/10.1016/j.bpj.2010.01.037

Hille, B. 1971. The permeability of the sodium channel to organic cations in myelinated nerve. *J. Gen. Physiol.* 58:599–619. https://doi.org/10.1085/jgp.58.6.599

Hille, B., A.M. Woodhull, and B.I. Shapiro. 1975. Negative surface charge near sodium channels of nerve: Divalent ions, monovalent ions, and pH. *Philos. Trans. R. Soc. Lond. B Biol. Sci.* 270:301–318. https://doi.org/10.1098/rstb.1975.0011

Hille, B., E.J. Dickson, M. Kruse, O. Vivas, and B.C. Suh. 2015. Phosphoinositides regulate ion channels. *Biochim. Biophys. Acta.* 1851:844–856. https://doi.org/10.1016/j.bbalip.2014.09.010

Hui, K., B. Liu, and F. Qin. 2003. Capsaicin activation of the pain receptor, VR1: Multiple open states from both partial and full binding. *Biophys. J.* 84:2957–2968. https://doi.org/10.1016/S0006-3495(03)70022-8

Inoue, M., M.H. Rashid, R. Fujita, J.J. Contos, J. Chun, and H. Ueda. 2004. Initiation of neuropathic pain requires lysophosphatidic acid receptor signaling. *Nat. Med.* 10:712–718. https://doi.org/10.1038/nm1060

Jans, R., L. Mottram, D.L. Johnson, A.M. Brown, S. Sikkink, K. Ross, and N.J. Reynolds. 2013. Lysophosphatidic acid promotes cell migration through STIM1- and Orai1-mediated Ca2+(i) mobilization and NFAT2 activation. *J. Invest. Dermatol.* 133:793–802. https://doi.org/10.1038/jid.2012.370

Jara-Oseguera, A., I. Llorente, T. Rosenbaum, and L.D. Islas. 2008. Properties of the inner pore region of TRPV1 channels revealed by block with quaternary ammoniums. *J. Gen. Physiol.* 132:547–562. https://doi.org/10.1085/jgp.200810051

Jara-Oseguera, A., C. Bae, and K.J. Swartz. 2016. An external sodium ion binding site controls allosteric gating in TRPV1 channels. *eLife.* 5:e13356. https://doi.org/10.7554/eLife.13356

Kittaka, H., K. Uchida, N. Fukuta, and M. Tominaga. 2017. Lysophosphatidic acid-induced itch is mediated by signalling of LPA$_5$ receptor, phospholipase D and TRPA1/TRPV1. *J. Physiol.* 595:2681–2698. https://doi.org/10.1113/JP273961

Koplas, P.A., R.L. Rosenberg, and G.S. Oxford. 1997. The role of calcium in the desensitization of capsaicin responses in rat dorsal root ganglion neurons. *J. Neurosci.* 17:3525–3537. https://doi.org/10.1523/JNEUROSCI.17-10-03525.1997

Kumar, N., P. Zhao, A. Tomar, C.A. Galea, and S. Khurana. 2004. Association of villin with phosphatidylinositol 4,5-bisphosphate regulates the actin cytoskeleton. *J. Biol. Chem.* 279:3096–3110. https://doi.org/10.1074/jbc.M308878200

Latorre, R., P. Labarca, and D. Naranjo. 1992. Surface charge effects on ion conduction in ion channels. *Methods Enzymol.* 207:471–501. https://doi.org/10.1016/0076-6879(92)07034-L

Latorre, R., S. Brauchi, G. Orta, C. Zaelzer, and G. Vargas. 2007. Thermo-TRP channels as modular proteins with allosteric gating. *Cell Calcium.* 42:427–438. https://doi.org/10.1016/j.ceca.2007.04.004

Liao, M., E. Cao, D. Julius, and Y. Cheng. 2013. Structure of the TRPV1 ion channel determined by electron cryo-microscopy. *Nature.* 504:107–112. https://doi.org/10.1038/nature12822

Liu, B., K. Hui, and F. Qin. 2003. Thermodynamics of heat activation of single capsaicin ion channels VR1. *Biophys. J.* 85:2988–3006. https://doi.org/10.1016/S0006-3495(03)74719-5

Liu, S., M. Umezu-Goto, M. Murph, Y. Lu, W. Liu, F. Zhang, S. Yu, L.C. Stephens, X. Cui, G. Murrow, et al. 2009. Expression of autotaxin and lysophosphatidic acid receptors increases mammary tumorigenesis, invasion, and metastases. *Cancer Cell.* 15:539–550. https://doi.org/10.1016/j.ccr.2009.03.027

Lundbaek, J.A., and O.S. Andersen. 1994. Lysophospholipids modulate channel function by altering the mechanical properties of lipid bilayers. *J. Gen. Physiol.* 104:645–673. https://doi.org/10.1085/jgp.104.4.645

Mergler, S., F. Garreis, M. Sahlmüller, P.S. Reinach, F. Paulsen, and U. Pleyer. 2011. Thermosensitive transient receptor potential channels in human corneal epithelial cells. *J. Cell. Physiol.* 226:1828–1842. https://doi.org/10.1002/jcp.22514

Morales-Lázaro, S.L., B. Serrano-Flores, I. Llorente, E. Hernández-García, R. González-Ramírez, S. Banerjee, D. Miller, V. Gududuru, J. Fells, D. Norman, et al. 2014. Structural determinants of the transient receptor potential 1 (TRPV1) channel activation by phospholipid analogs. *J. Biol. Chem.* 289:24079–24090. https://doi.org/10.1074/jbc.M114.572503

Nieto-Posadas, A., G. Picazo-Juárez, I. Llorente, A. Jara-Oseguera, S. Morales-Lázaro, D. Escalante-Alcalde, L.D. Islas, and T. Rosenbaum. 2012. Lysophosphatidic acid directly activates TRPV1 through a C-terminal binding site. *Nat. Chem. Biol.* 8:78–85. https://doi.org/10.1038/nchembio.712

Oldham, K.B. 2008. A Gouy–Chapman–Stern model of the double layer at a (metal)/(ionic liquid) interface. *J. Electroanal. Chem.* 613:131–138. https://doi.org/10.1016/j.jelechem.2007.10.017

Oseguera, A.J., L.D. Islas, R. García-Villegas, and T. Rosenbaum. 2007. On the mechanism of TBA block of the TRPV1 channel. *Biophys. J.* 92:3901–3914. https://doi.org/10.1529/biophysj.106.102400

Park, J.B., H.J. Kim, P.D. Ryu, and E. Moczydlowski. 2003. Effect of phosphatidylserine on unitary conductance and Ba2+ block of the BK Ca2+-activated K+ channel: Re-examination of the surface charge hypothesis. *J. Gen. Physiol.* 121:375–398. https://doi.org/10.1085/jgp.200208746

Rosenbaum, T., and S.E. Gordon. 2002. Dissecting intersubunit contacts in cyclic nucleotide-gated ion channels. *Neuron.* 33:703–713. https://doi.org/10.1016/S0896-6273(02)00599-8

Samways, D.S., and T.M. Egan. 2011. Calcium-dependent decrease in the single-channel conductance of TRPV1. *Pflugers Arch.* 462:681–691. https://doi.org/10.1007/s00424-011-1013-7

Schumacher, K.A., H.G. Classen, and M. Späth. 1979. Platelet aggregation evoked in vitro and in vivo by phosphatidic acids and lysoderivatives: Identity with substances in aged serum (DAS). *Thromb. Haemost.* 42:631–640. https://doi.org/10.1055/s-0038-1666902

Sheng, X., Y.C. Yung, A. Chen, and J. Chun. 2015. Lysophosphatidic acid signalling in development. *Development.* 142:1390–1395. https://doi.org/10.1242/dev.121723

Sigworth, F.J., and S.M. Sine. 1987. Data transformations for improved display and fitting of single-channel dwell time histograms. *Biophys. J.* 52:1047–1054. https://doi.org/10.1016/S0006-3495(87)83298-8

Sprong, H., P. van der Sluijs, and G. van Meer. 2001. How proteins move lipids and lipids move proteins. *Nat. Rev. Mol. Cell Biol.* 2:504–513. https://doi.org/10.1038/35080071

Stirling, L., M.R. Williams, and A.D. Morielli. 2009. Dual roles for RHOA/RHO-kinase in the regulated trafficking of a voltage-sensitive potassium channel. *Mol. Biol. Cell.* 20:2991–3002. https://doi.org/10.1091/mbc.e08-10-1074

Thompson, J., and T. Begenisich. 2000. Interaction between quaternary ammonium ions in the pore of potassium channels. Evidence against an electrostatic repulsion mechanism. *J. Gen. Physiol.* 115:769–782. https://doi.org/10.1085/jgp.115.6.769

Ufret-Vincenty, C.A., R.M. Klein, L. Hua, J. Angueyra, and S.E. Gordon. 2011. Localization of the PIP2 sensor of TRPV1 ion channels. *J. Biol. Chem.* 286:9688–9698. https://doi.org/10.1074/jbc.M110.192526

van Corven, E.J., A. Groenink, K. Jalink, T. Eichholtz, and W.H. Moolenaar. 1989. Lysophosphatidate-induced cell proliferation: Identification and dissection of signaling pathways mediated by G proteins. *Cell.* 59:45–54. https://doi.org/10.1016/0092-8674(89)90868-4

Yamada, T., K. Sato, M. Komachi, E. Malchinkhuu, M. Tobo, T. Kimura, A. Kuwabara, Y. Yanagita, T. Ikeya, Y. Tanahashi, et al. 2004. Lysophosphatidic acid (LPA) in malignant ascites stimulates motility of human pancreatic cancer cells through LPA1. *J. Biol. Chem.* 279:6595–6605. https://doi.org/10.1074/jbc.M308133200

Yung, Y.C., N.C. Stoddard, and J. Chun. 2014. LPA receptor signaling: Pharmacology, physiology, and pathophysiology. *J. Lipid Res.* 55:1192–1214. https://doi.org/10.1194/jlr.R046458